Low-Q^2 L/T-Separated Cross Sections and Pion Form Factor Results from PionLT (E12-19-006)

Vijay Kumar

University of Regina

January 26, 2026

Charged Meson Form Factors

Simple $q\bar{q}$ valence structure of mesons presents the ideal testing ground for our understanding of bound quark systems.

In quantum field theory, the form factor is the overlap integral:

$$F_\pi(Q^2) = \int \phi_\pi^*(p)\phi_\pi(p+q)dp$$

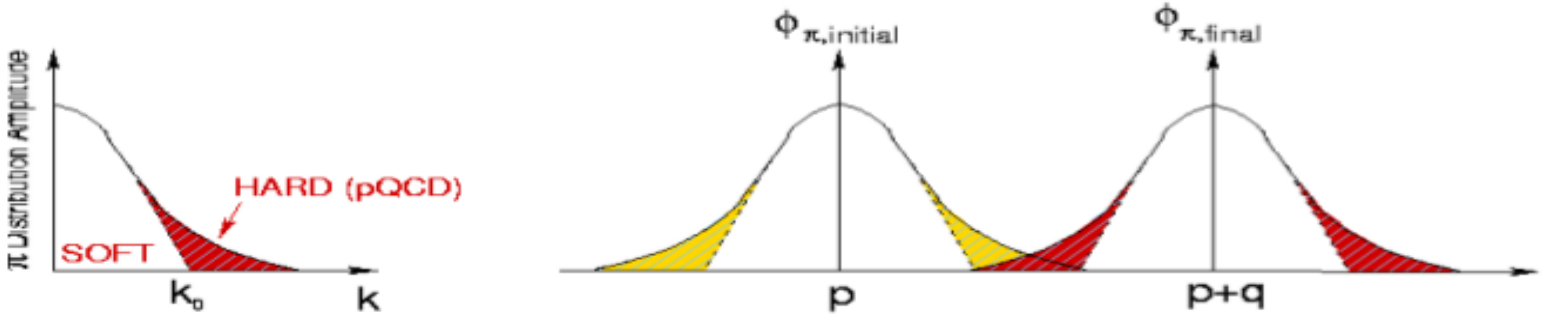

The meson wave function can be separated into φ_π^{soft} with only low momentum contributions ($k<k_0$) and a hard tail φ_π^{hard}.

While φ_π^{hard} can be treated in pQCD, φ_π^{soft} cannot.

From a theoretical standpoint, the study of the Q^2–dependence of the form factor focuses on finding a description for the hard and soft contributions of the meson wave-function.

π^+ Form Factor – Low Q^2 (Direct Measurement)

At low Q^2, F_π can be measured model–independently via high energy elastic π^- scattering from atomic electrons in Hydrogen

- CERN SPS used 300 GeV pions to measure form factor up to $Q^2 = 0.25$ GeV^2 *[Amendolia, et al., NPB **277**(1986)168]*

- Data used to extract pion charge radius $r_\pi = 0.657 \pm 0.012$ fm

Maximum accessible Q^2 roughly proportional to pion beam energy

Q^2=1 GeV^2 requires 1 TeV pion beam

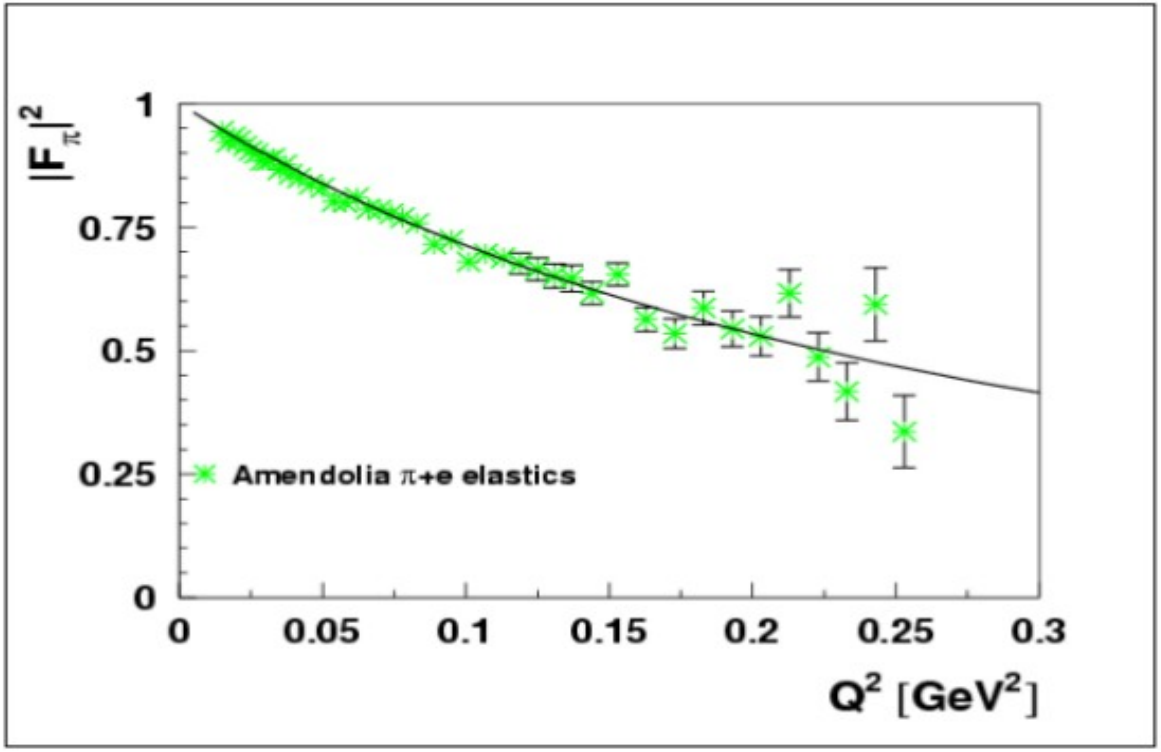

π^+ Form Factor via Electroproduction (Indirect Technique)

Above Q^2>0.3 GeV^2, F_π is measured indirectly using the "pion cloud" of the proton via pion electroproduction $p(e,e'\pi^+)n$

$$|p\rangle = |p\rangle_0 + |n\pi^+\rangle + \ldots$$

- At small $-t$, the pion pole process dominates the longitudinal cross section, σ_L
- In Born term model, F_π^2 appears as

$$\frac{d\sigma_L}{dt} \propto \frac{-tQ^2}{(t-m_\pi^2)}\, g_{\pi NN}^2(t)\, F_\pi^2(Q^2,t)$$

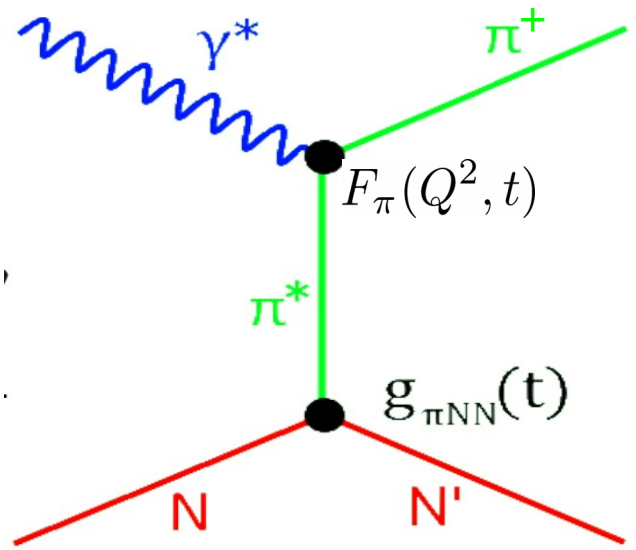

Drawbacks of this technique:

1. Isolating σ_L experimentally challenging.
2. The F_π values are in principle dependent upon the model used, but this dependence is expected to be reduced at sufficiently small $-t$.

My Ph.D. research aims to improve understanding of the indirect technique by analyzing low-Q^2 data and comparing it with direct measurements.

Rosenbluth (L/T) Separation Technique

$$2\pi\frac{d^2\sigma}{dtd\phi}=\varepsilon\frac{d\sigma_L}{dt}+\frac{d\sigma_T}{dt}+\sqrt{2\varepsilon(\varepsilon+1)}\frac{d\sigma_{LT}}{dt}\cos\phi+\varepsilon\frac{d\sigma_{TT}}{dt}\cos 2\phi$$

Virtual-photon polarization:

$$\varepsilon=\left(1+2\frac{(E_e-E_{e'})^2+Q^2}{Q^2}\tan^2\frac{\theta_{e'}}{2}\right)^{-1}$$

$$e+p\rightarrow e'+\pi^+ +n$$

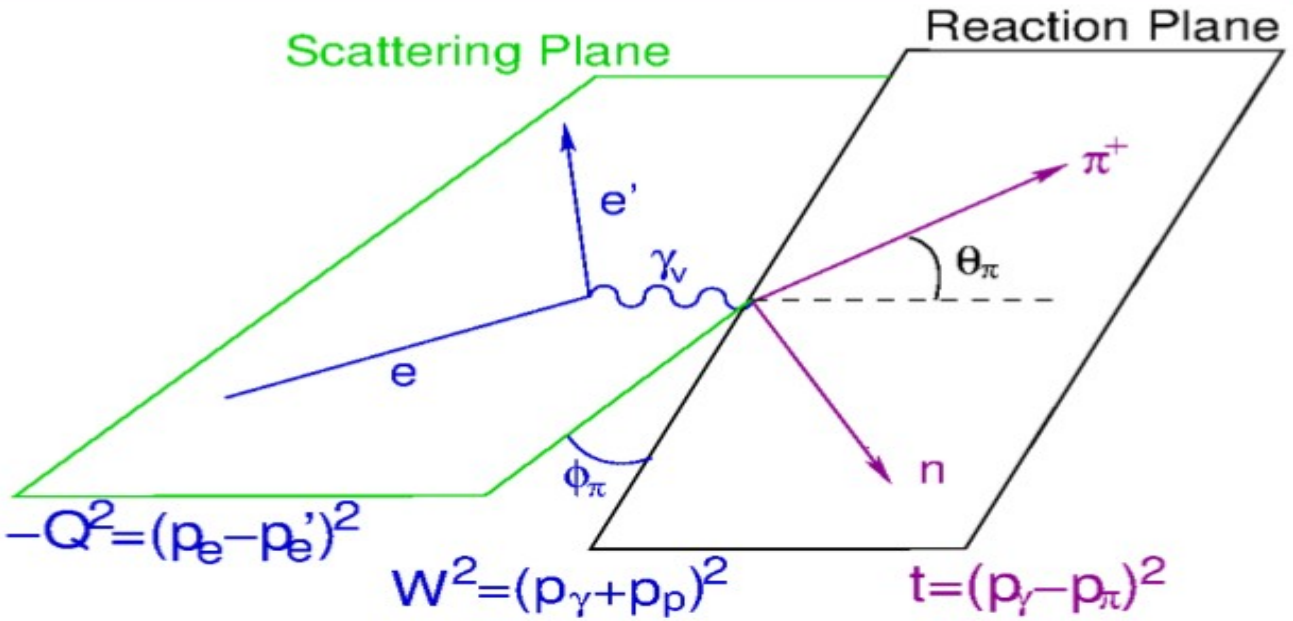

- **L-T separation required to separate σ_L from σ_T**
- **Need to take data at smallest available $-t$, so σ_L has maximum contribution from the π^+ pole**
- **Need to measure t–dependence of σ_L at fixed Q^2,W**

E12-19-006 Experiment

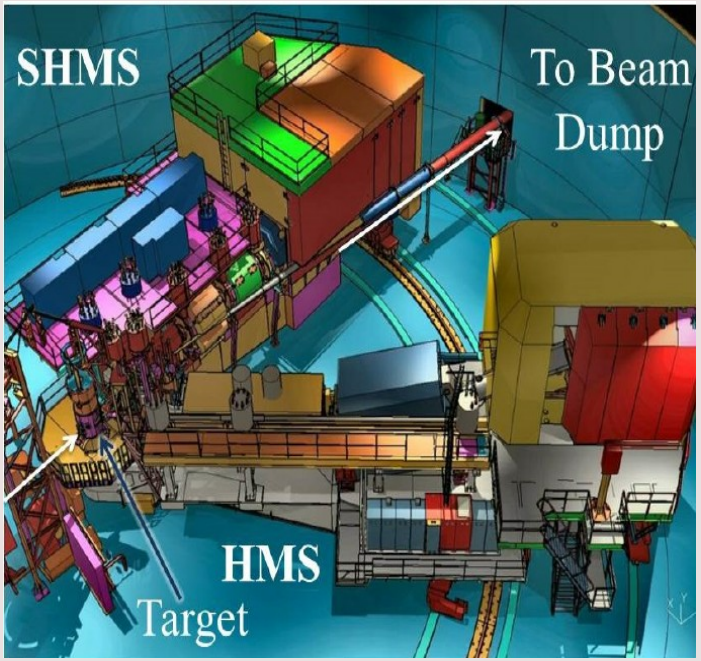

- The experiment conducted in three phases,
  - **First run period:** ran in summer 2019 – analyzed by me
  - **Second run period:** ran in fall 2021
  - **Third run period:** ran in fall 2022
- The reaction system

$$e + p \rightarrow e' + \pi^+ + n$$

SHMS

HMS

- Spokesperson
  - Dr. Garth Huber (UofR), Dr. Tanja Horn (CUA), and Dr. David Gaskell (JLab)

E12-19-006 Experiment – First Run Data

$Q^2 = 0.38$ GeV^2, $W = 2.20$ GeV, $-t = 0.008$ GeV^2								
$E_b = 2.7$ GeV, $\epsilon_1 = 0.286$			$E_b = 3.6$ GeV, $\epsilon_2 = 0.629$			$E_b = 4.5$ GeV, $\epsilon_3 = 0.781$		
Spectrometer Angle ($\theta°$)			Spectrometer Angle ($\theta°$)			Spectrometer Angle ($\theta°$)		
SHMS	HMS	Setting	SHMS	HMS	Setting	SHMS	HMS	Setting
5.70	31.965	Center	5.75	15.83	Right2	7.645	10.965	Right1
7.695	31.965	Left1	6.87	15.83	Right1	10.325	10.965	Center
9.705	31.965	Left2	8.87	15.83	Center	12.34	10.965	Left1
-	-	N/A	10.87	15.83	Left1	14.325	10.965	Left2
-	-	N/A	12.87	15.83	Left2	-	-	N/A

$Q^2 = 0.375$ GeV^2

LOW ε: 3 SHMS SETTINGS

MIDDLE ε: 5 SHMS SETTINGS

HIGH ε: 4 SHMS SETTINGS

Total = 12 SHMS Settings

$Q^2 = 0.42$ GeV^2, $W = 2.20$, $-t = 0.010$ GeV^2								
$E_b = 2.7$ GeV, $\epsilon_1 = 0.264$			$E_b = 3.6$ GeV, $\epsilon_2 = 0.617$			$E_b = 4.5$ GeV, $\epsilon_3 = 0.774$		
Spectrometer Angle ($\theta°$)			Spectrometer Angle ($\theta°$)			Spectrometer Angle ($\theta°$)		
SHMS	HMS	Setting	SHMS	HMS	Setting	SHMS	HMS	Setting
5.70	35.19	Center	9.200	17.025	Center	6.870	11.745	Right2
7.75	35.175	Left1	11.20	17.025	Left1	8.075	11.745	Right1
9.740	35.175	Left2	13.20	17.025	Left2	10.075	11.745	Center
-	-	N/A	-	-	N/A	12.075	11.745	Left1
-	-	N/A	-	-	N/A	14.08	11.745	Left2

$Q^2 = 0.425$ GeV^2

LOW ε: 3 SHMS SETTINGS

MIDDLE ε: 3 SHMS SETTINGS

HIGH ε: 5 SHMS SETTINGS

Total = 11 SHMS Settings

Yield Correction Factors – Key for L/T Separation

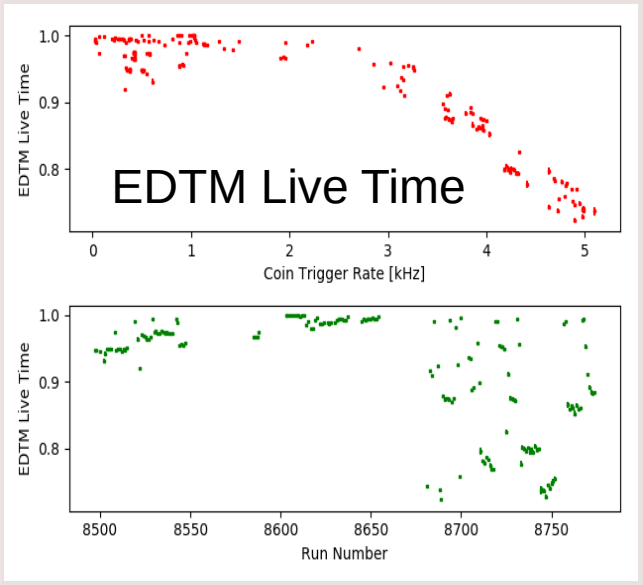

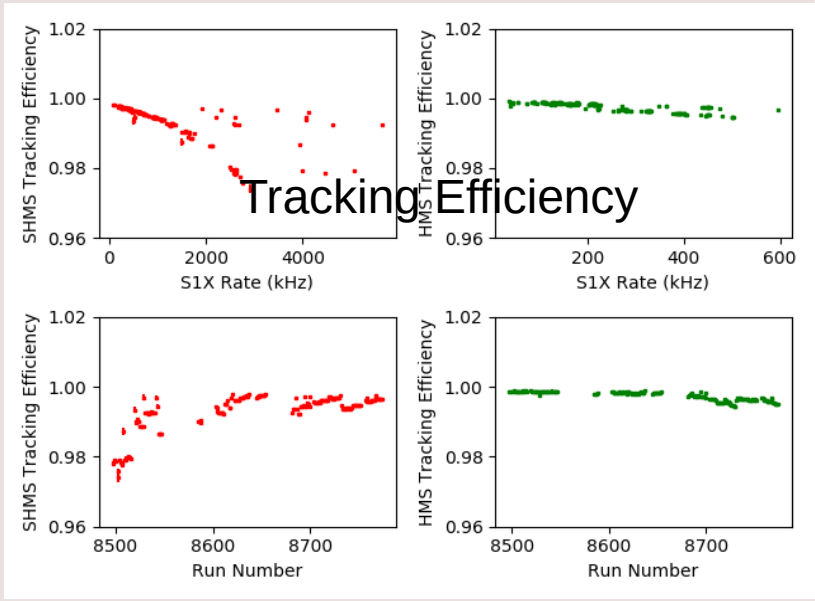

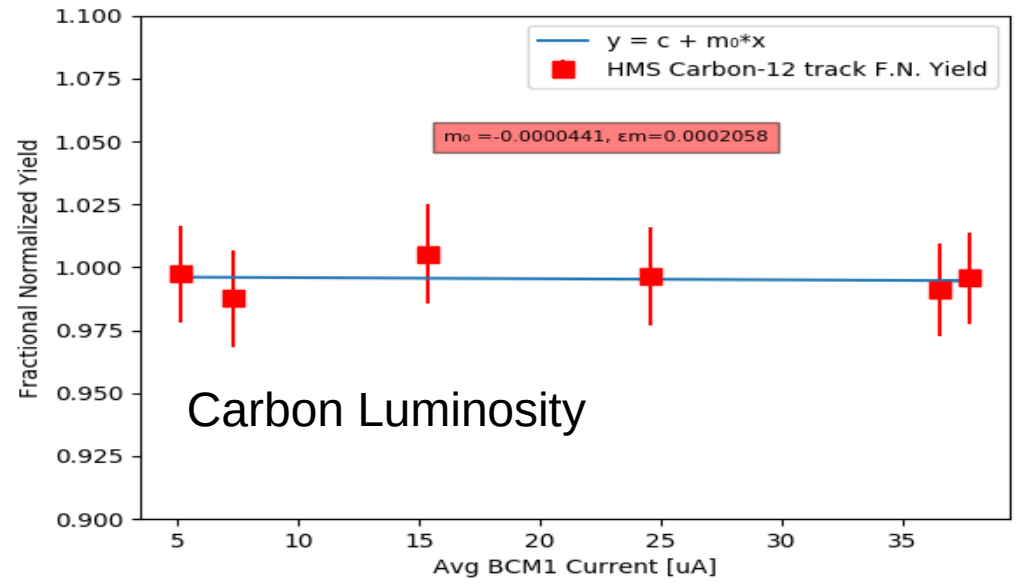

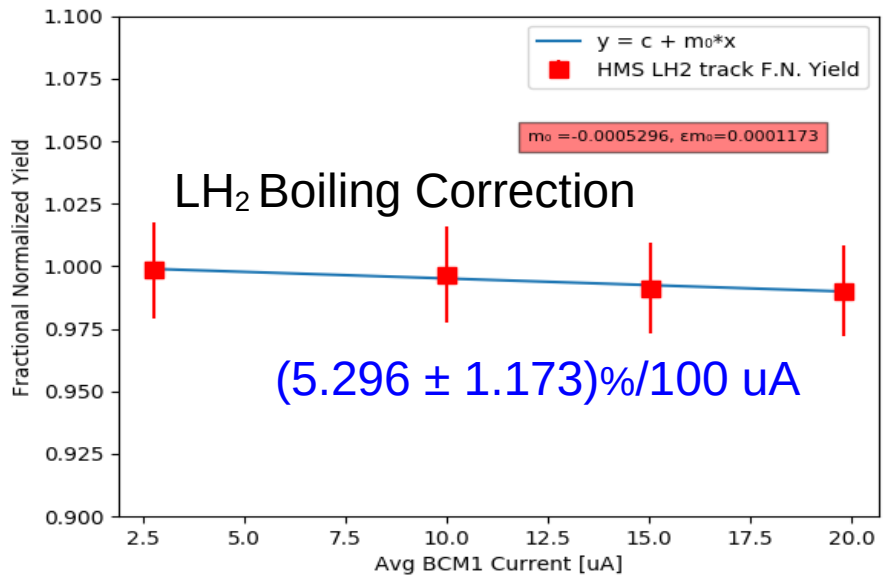

Yield Correction Factors – Key for L/T Separation

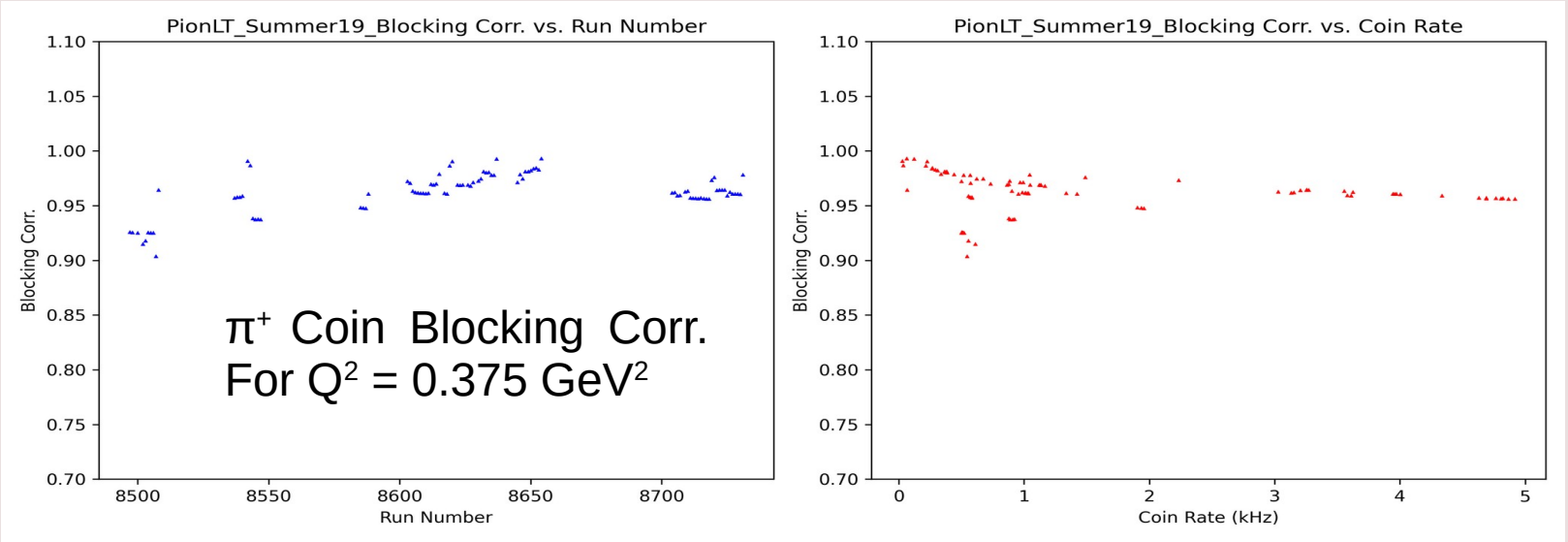

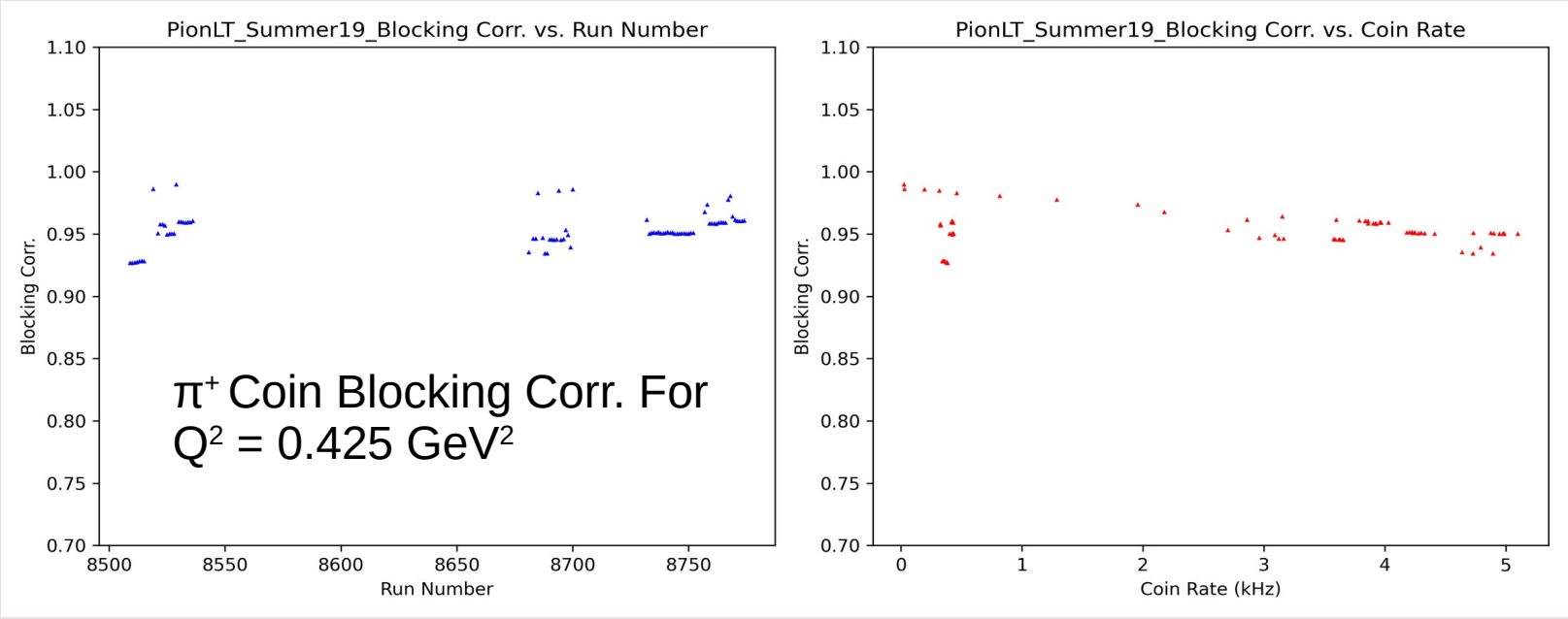

‘Heep’, $e + p \rightarrow e' + p$, Analysis – Kinematic Offsets & Elastic X-Section

- For the LT separation, the beam energy, spectrometer angles, and momenta obtained from power-supply calibrations and floor-angle markings were not sufficiently precise.
  - The Heep reaction is kinematically over-determined, with both the scattered electron (e’) and the proton detected.
  - We used the deviations between observed and physically required values to determine the experimental offsets.

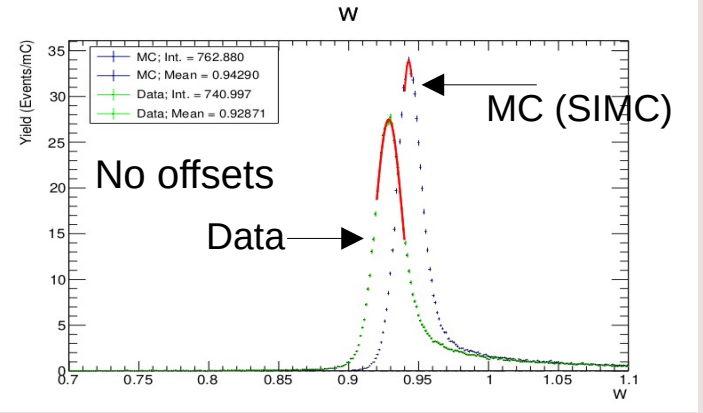

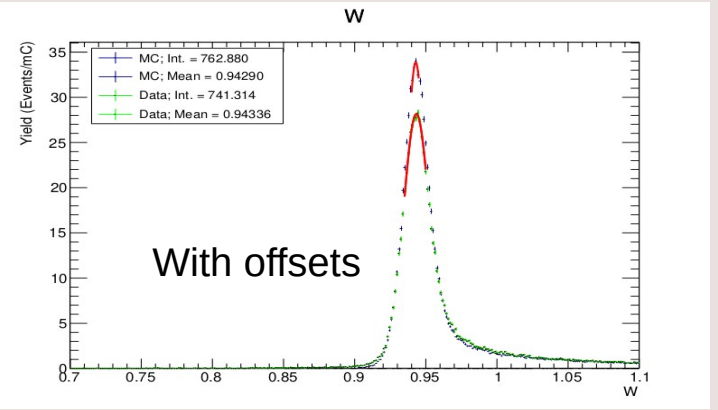

- Elastic X-Section

$$Yield = \frac{N}{Q_{tot} \times \epsilon_{tot}}$$

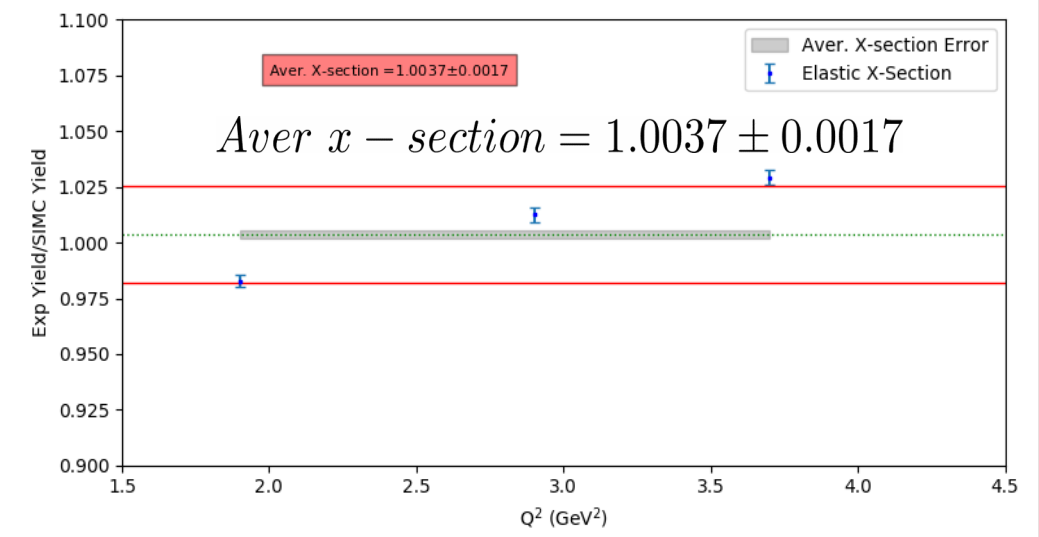

For Q^2 = 0.375 and 0.425 GeV² L/T Analysis →

Quantity	SHMS	HMS
In-plane angle	2.8 mrad	1.2 mrad
Out-of-plane angle	0.0	0.99 mrad
Central Momentum	0.0	0.15%
Beam Energy	0.01% to 0.07%	

$e + p \rightarrow e' + \pi^+ + n$ Event Selection: π^+ & e^- Coincidence Time

- The coincidence time was used to select clean π^+–e^- events for the analysis. Random coincidences were subtracted by selecting random beam buckets and normalizing to the width of the prompt peak (2 ns).

$$t_{coin} = t_{HMS} - t_{SHMS}$$

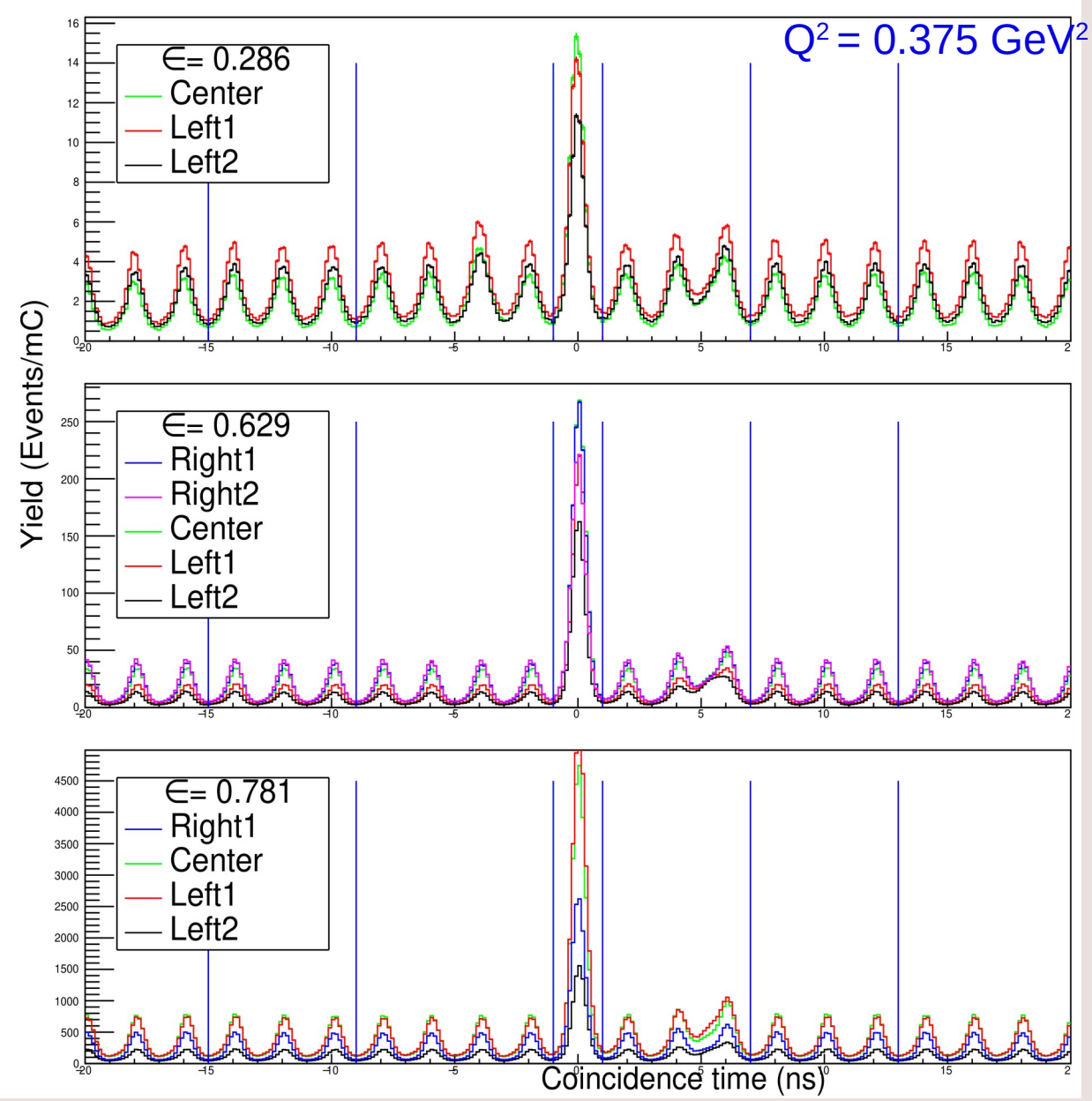

$e + p \rightarrow e' + \pi^+ + n$ Exclusive Final State: π^+ Missing Mass

Plot: Mid ε, Center Setting
of Q^2 = 0.375 GeV^2 data

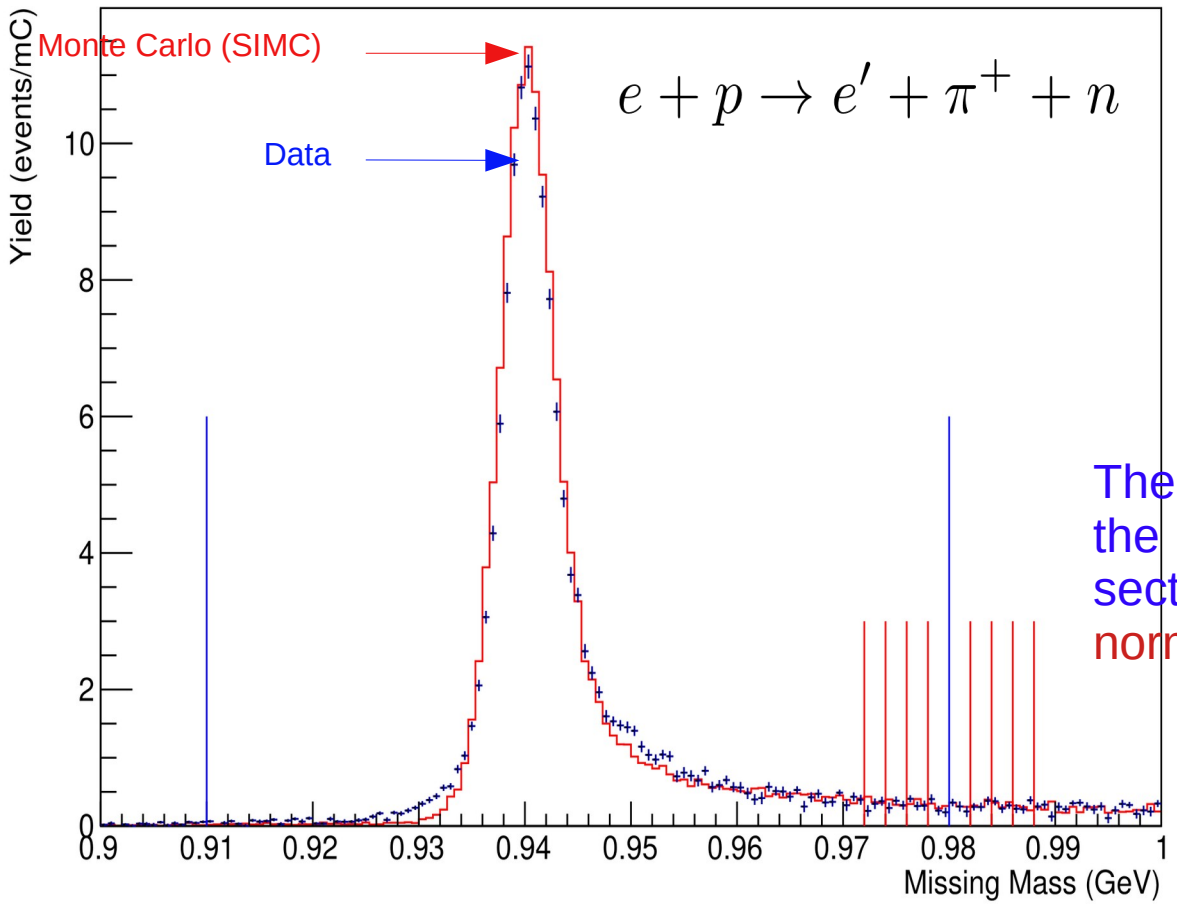

The exclusive π^+ final state was uniquely identified using the missing mass technique.

The red distribution represents the MC (SIMC) predicted cross section, not arbitrarily normalized to the data.

$$MM = \sqrt{((E_b + m_p - E'_e - E_{\pi^+})^2 - (\vec{P}_e - \vec{P}_{e'} - \vec{P}_{\pi^+})^2)}$$

$e + p \rightarrow e' + \pi^+ + n$ Diamond Cut

$Q^2 = 0.375\ GeV^2$

- The absolute acceptance of the spectrometers depends on the beam energy or ε settings.
- To ensure uniform acceptance for the LT separation across all ε settings, a cut called the ‘diamond cut’ is applied.

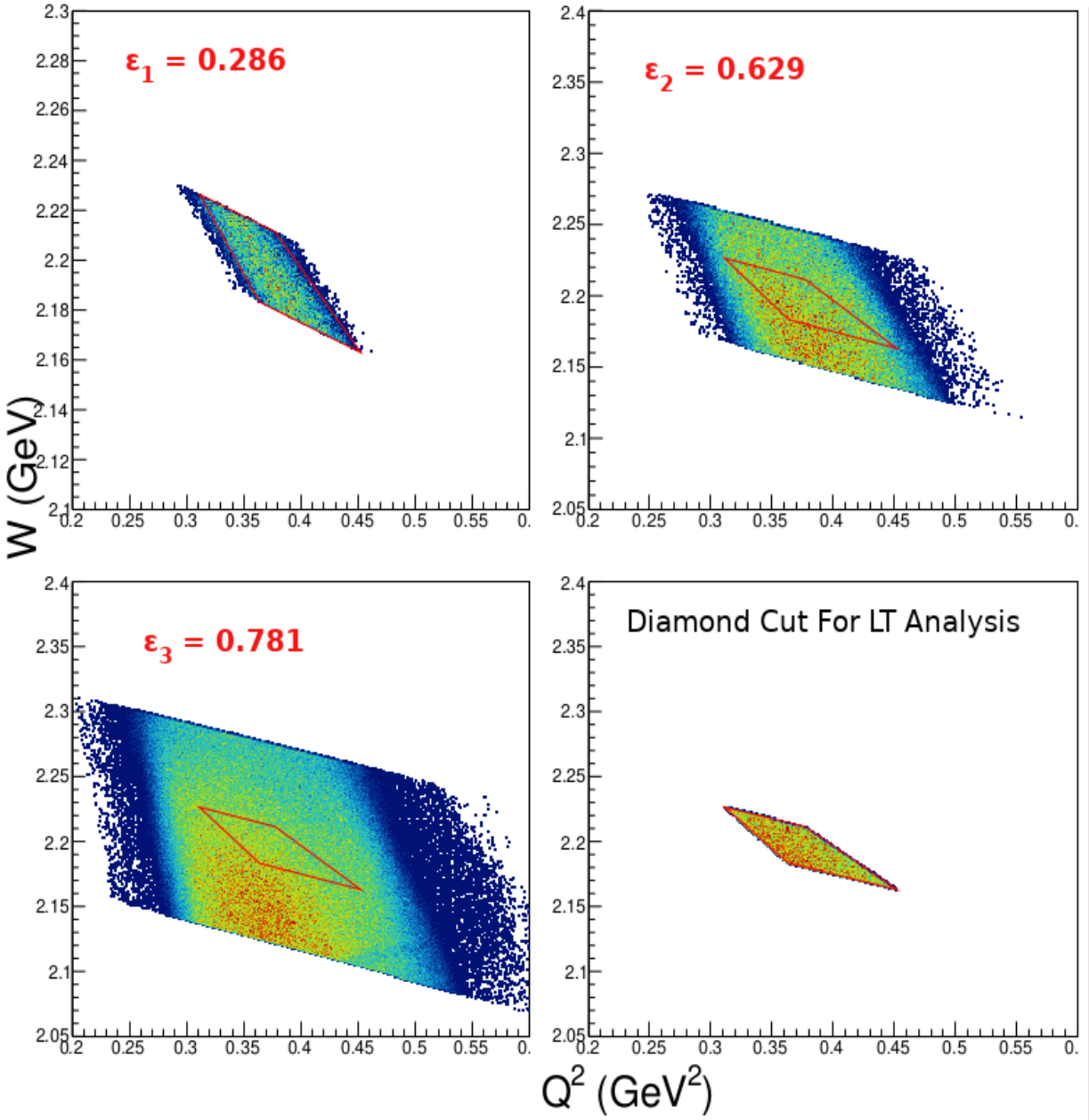

$e + p \rightarrow e' + \pi^+ + n$ Binning in t and φ Angles

$Q^2 = 0.375\ GeV^2$

- The data were binned in t to measure the individual π^+ separated cross-section as a function of t.
- Each t bin was further divided into 16 φ bins, enabling better simultaneous fitting using the Rosenbluth separation technique to extract the individual separated cross sections.

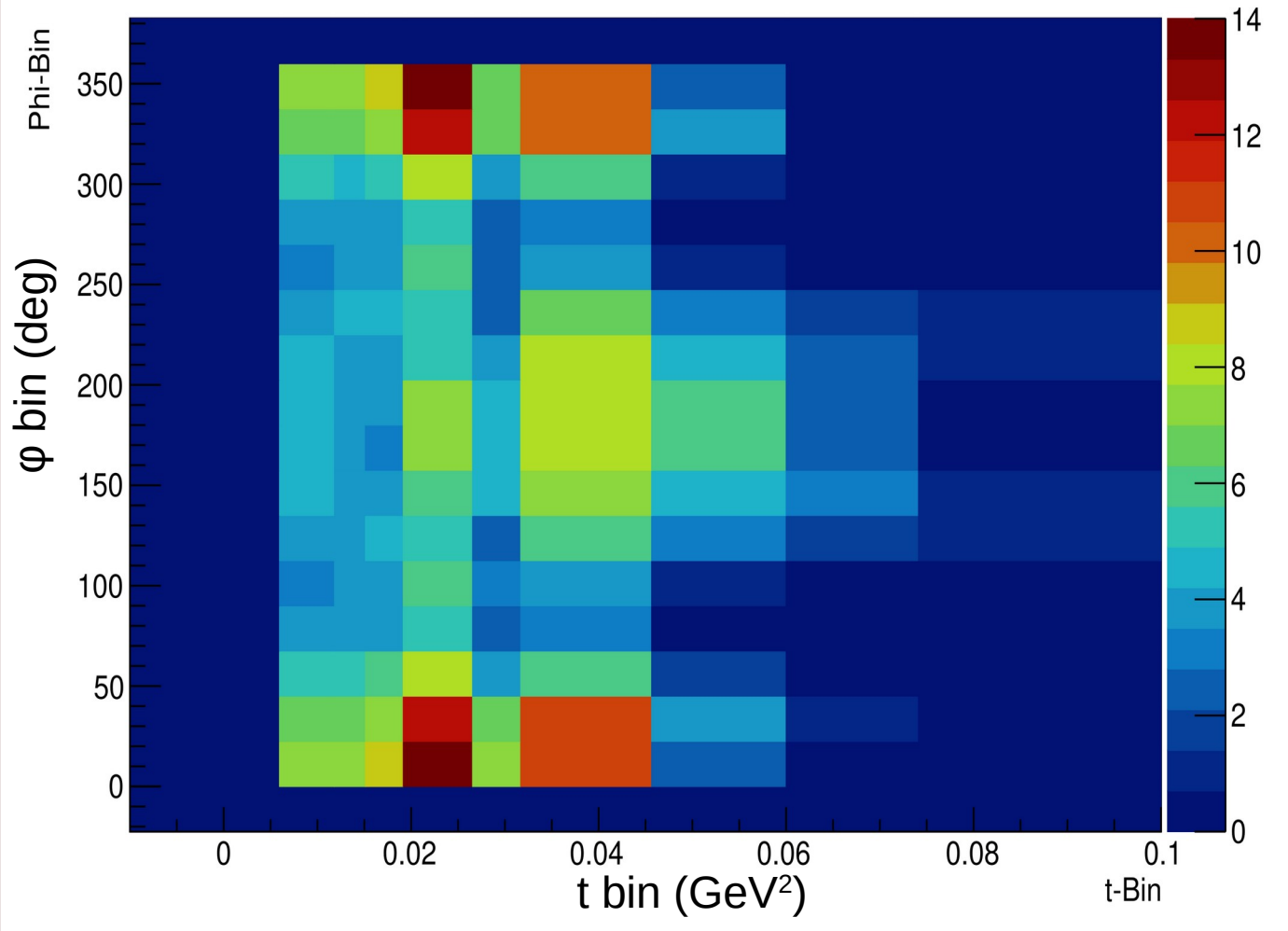

$$t = (p_\gamma - p_\pi)^2$$

$e + p \rightarrow e' + \pi^+ + n$ Experimental X-Section (Iterative Procedure)

For each ε, SHMS settings were analyzed separately to form yield ratios, which were then combined using error-weighted averaging with propagated uncertainties.

$$R = \frac{Yield_{\exp}}{Yield_{MC}}$$

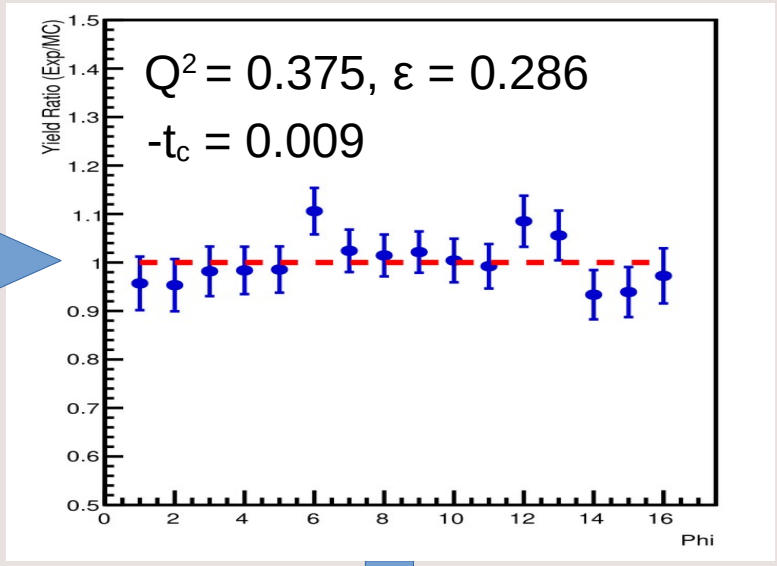

Fit models to σ_L, σ_T, σ_{LT} & σ_{TT} to determine an updated set of parameters.

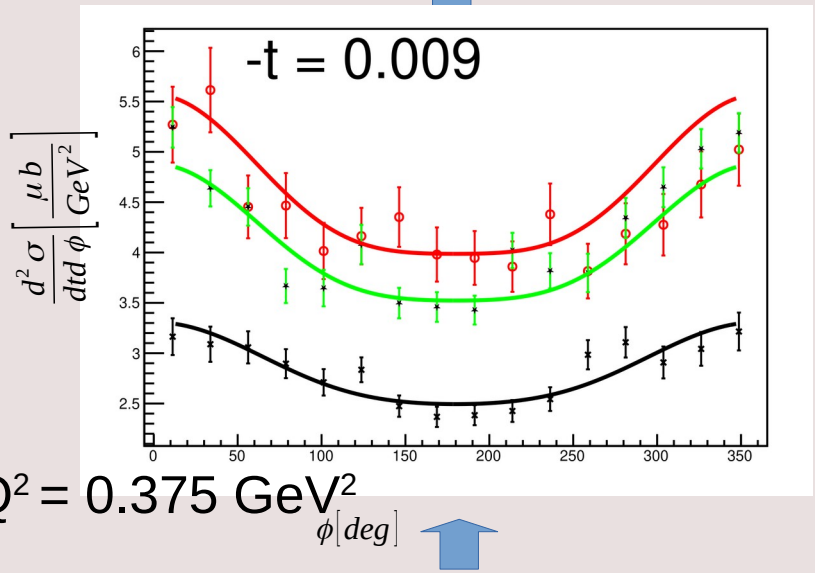

$$\sigma_{exp}(\bar{W}, \bar{Q^2}, t, \phi; \bar{\theta}, \bar{\epsilon}) = \frac{Y_{exp}}{Y_{MC}} \sigma_{MC}(\bar{W}, \bar{Q^2}, t, \phi; \bar{\theta}, \bar{\epsilon}).$$

$$2\pi \frac{d^2\sigma}{dtd\phi} = \epsilon \frac{d\sigma_L}{dt} + \frac{d\sigma_T}{dt} + \sqrt{2\epsilon(\epsilon+1)} \frac{d\sigma_{LT}}{dt} cos\phi + \epsilon \frac{d\sigma_{TT}}{dt} cos2\phi$$

Data vs. SIMC: Yield Comparison of Acceptance Variables

$$e + p \rightarrow e' + \pi^+ + n$$

Data

Monte Carlo (SIMC)

- To verify SIMC acceptance, experimental and SIMC acceptance variables were compared. The red distribution shows MC-predicted cross sections after the final iteration, not arbitrarily normalized to data.

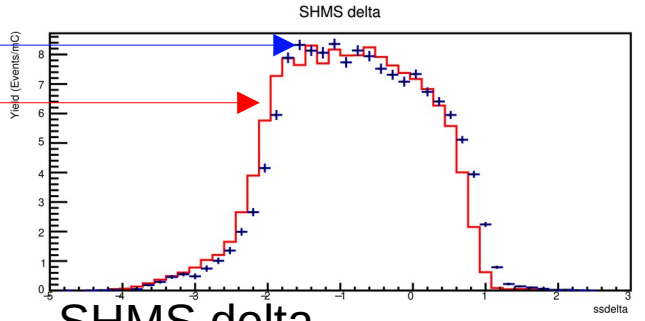

SHMS delta

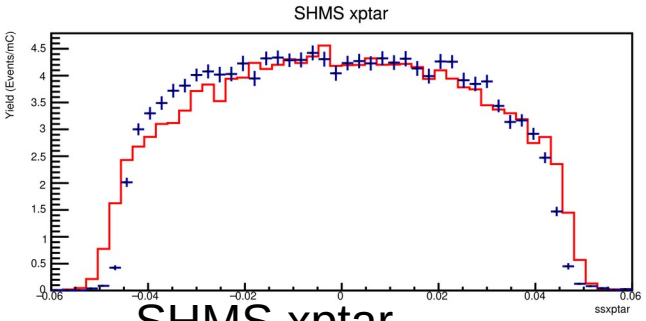

SHMS xptar

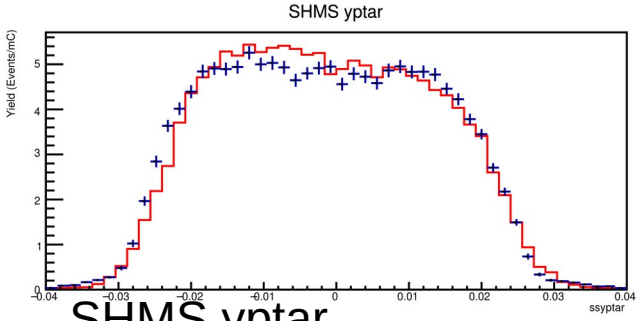

SHMS yptar

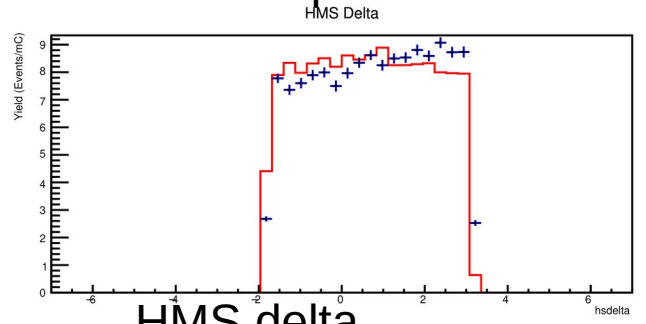

HMS delta

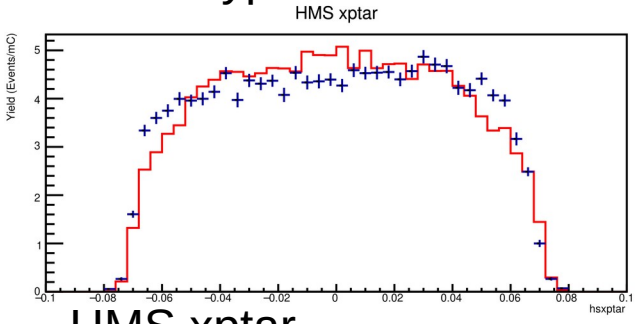

HMS xptar

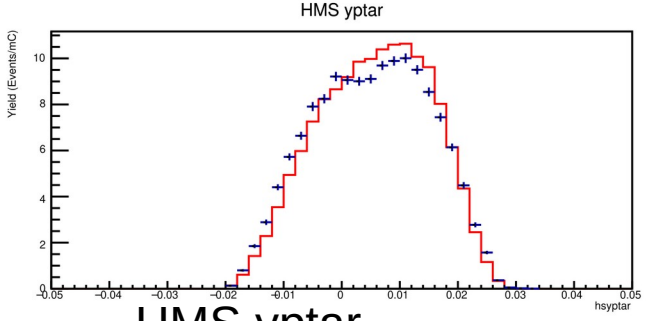

HMS yptar

Plot: Mid ε, Center Setting of Q^2 = 0.375 GeV^2 data

Data vs. SIMC: Yield Comparison of Kinematic Variables

$$e + p \rightarrow e' + \pi^+ + n$$

- To verify SIMC Kinematic, experimental and SIMC Kinematic variables were compared. The red distribution shows MC-predicted cross sections after the final iteration, not arbitrarily normalized to data.

Monte Carlo (SIMC)

Data

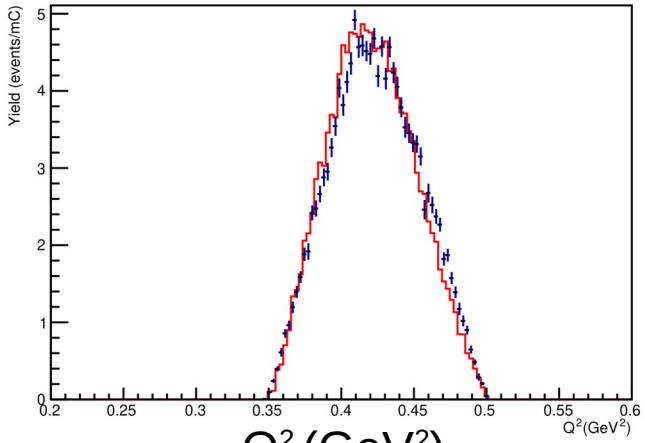

Q^2 (GeV^2)

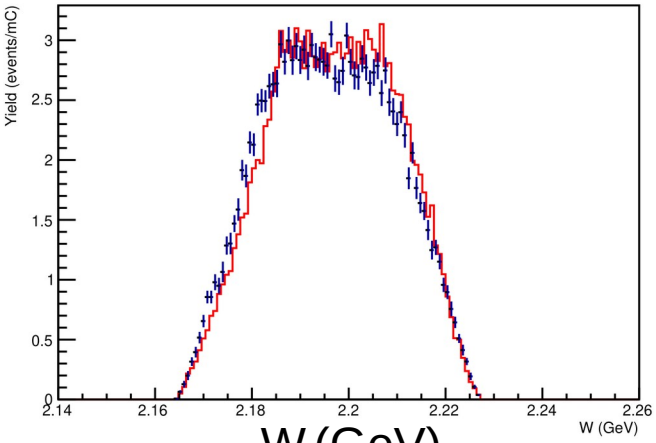

W (GeV)

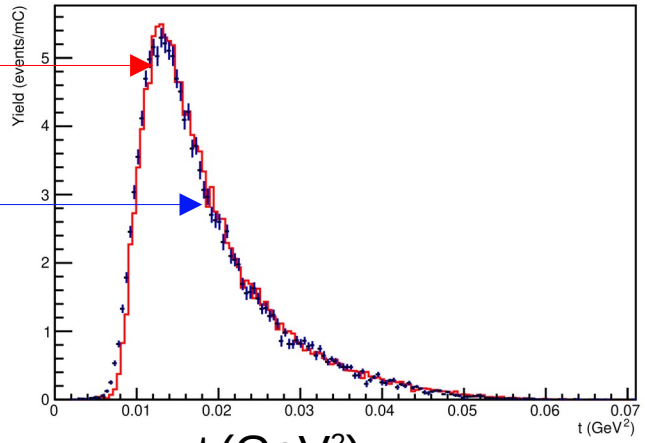

t (GeV^2)

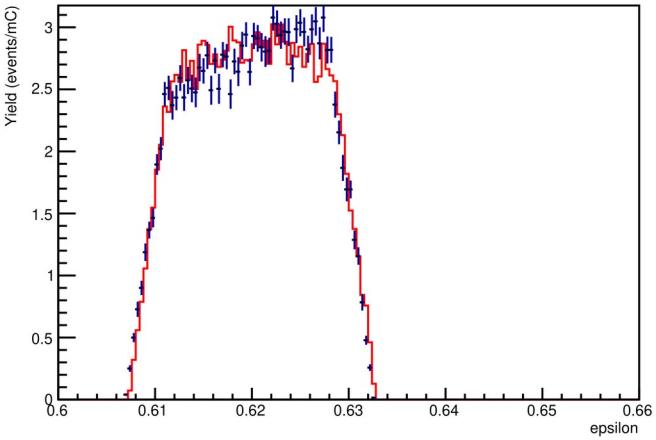

ε

Plot: Mid ε, Center Setting of Q^2 = 0.375 GeV^2 data

Unseparated X-Sections

$$e + p \rightarrow e' + \pi^+ + n$$

- Simultaneous fit of all 7 t bins at Q^2 = 0.375 GeV^2 using the Rosenbluth separation technique to measure individual separated cross sections.

$$2\pi \frac{d^2\sigma}{dtd\phi} = \epsilon \frac{d\sigma_L}{dt} + \frac{d\sigma_T}{dt} + \sqrt{2\epsilon(\epsilon+1)} \frac{d\sigma_{LT}}{dt} cos\phi + \epsilon \frac{d\sigma_{TT}}{dt} cos2\phi$$

- **High ε = 0.781**
- **Middle ε = 0.629**
- **Low ε = 0.286**

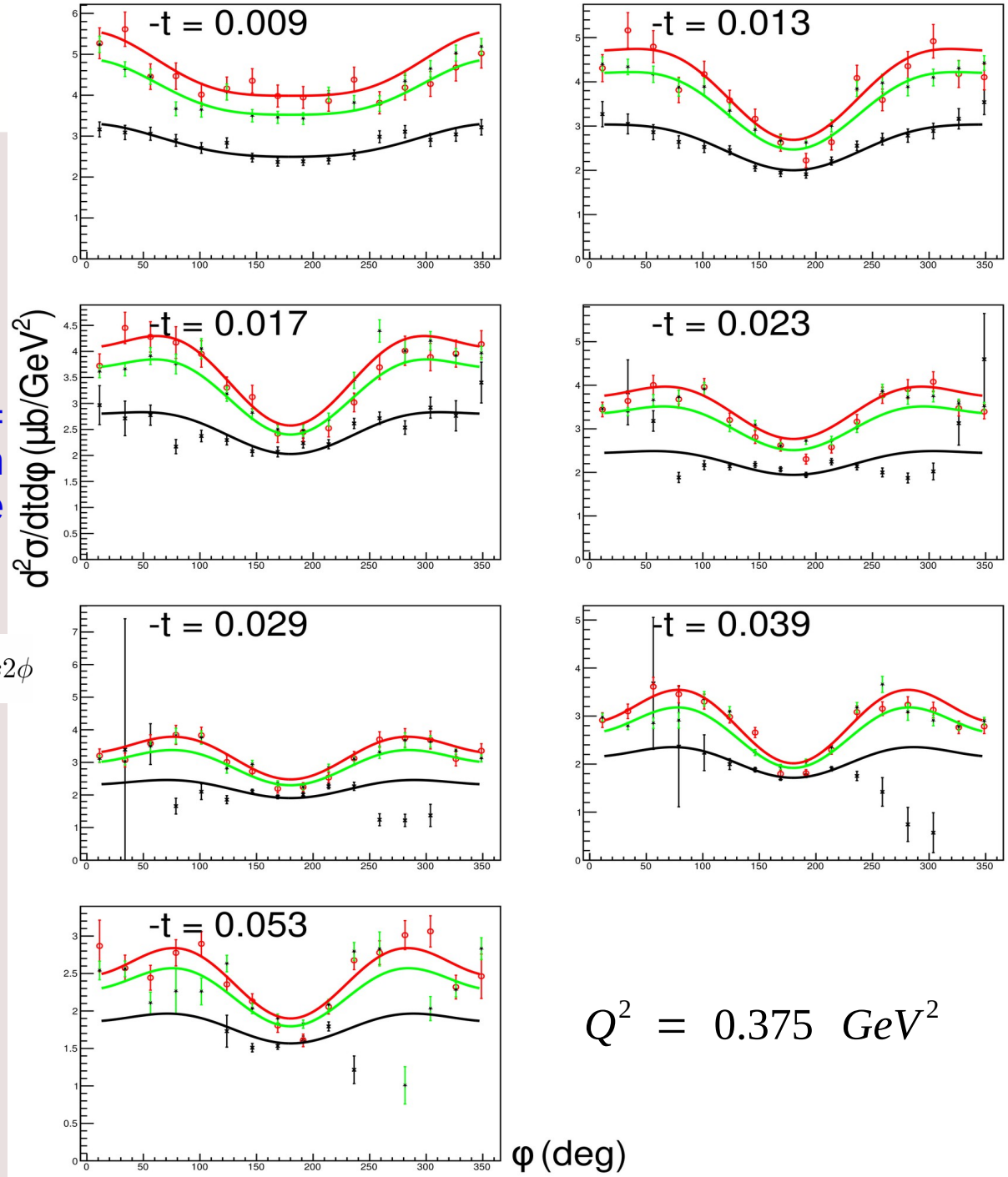

$$Q^2 = 0.375 \ GeV^2$$

Unseparated X-Sections

$$e + p \rightarrow e' + \pi^+ + n$$

- Simultaneous fit of all 7 t bins at Q^2 = 0.425 GeV^2 using the Rosenbluth separation technique to measure individual separated cross sections.

$$2\pi \frac{d^2\sigma}{dtd\phi} = \epsilon \frac{d\sigma_L}{dt} + \frac{d\sigma_T}{dt} + \sqrt{2\epsilon(\epsilon+1)} \frac{d\sigma_{LT}}{dt} cos\phi + \epsilon \frac{d\sigma_{TT}}{dt} cos2\phi$$

- **High ε = 0.774**
- **Middle ε = 0.617**
- **Low ε = 0.264**

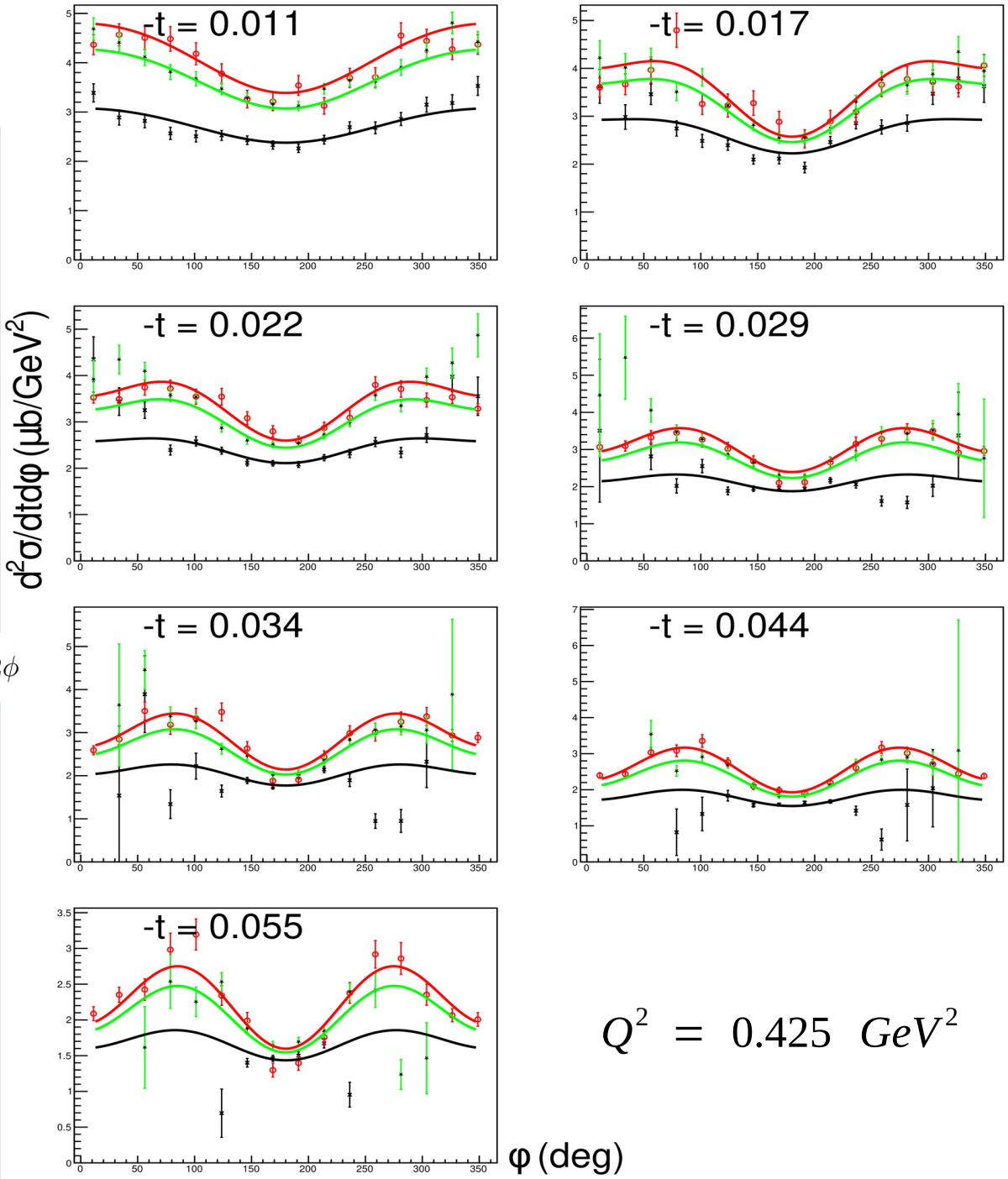

$$Q^2 = 0.425 \ GeV^2$$

Separated X-Sections at Q^2 = 0.375 GeV²

$$e + p \rightarrow e' + \pi^+ + n$$

- Separated cross sections for seven t bins obtained from a simultaneous fit using the Rosenbluth separation technique.

- Ackermann results rescaled to my kinematics for direct comparison (approximate).

VGL Regge model calculation over the t-bin range.

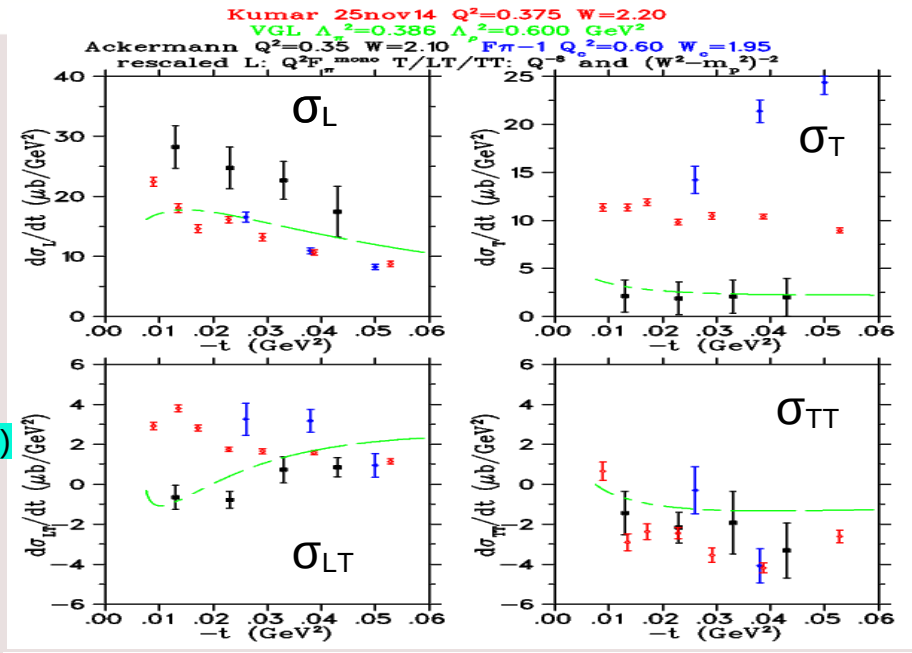

VGL, Phys. Rev. C 57, 1454 (1998)

New Findings:

- At Q^2 = 0.35 GeV², the Ackermann extraction of σ_{LT} differs in sign, while my results are consistent with the Fπ-1 analysis.

- The VGL model underestimates the σ_T contribution; the CKY model improves the description but does not fully reproduce the data.

- My results and the earlier Fπ-1 analysis show significantly higher σ_T than Ackermann, consistent with the substantial unseparated cross section observed at low ε.

CKY Regge model calculation over the t-bin range.

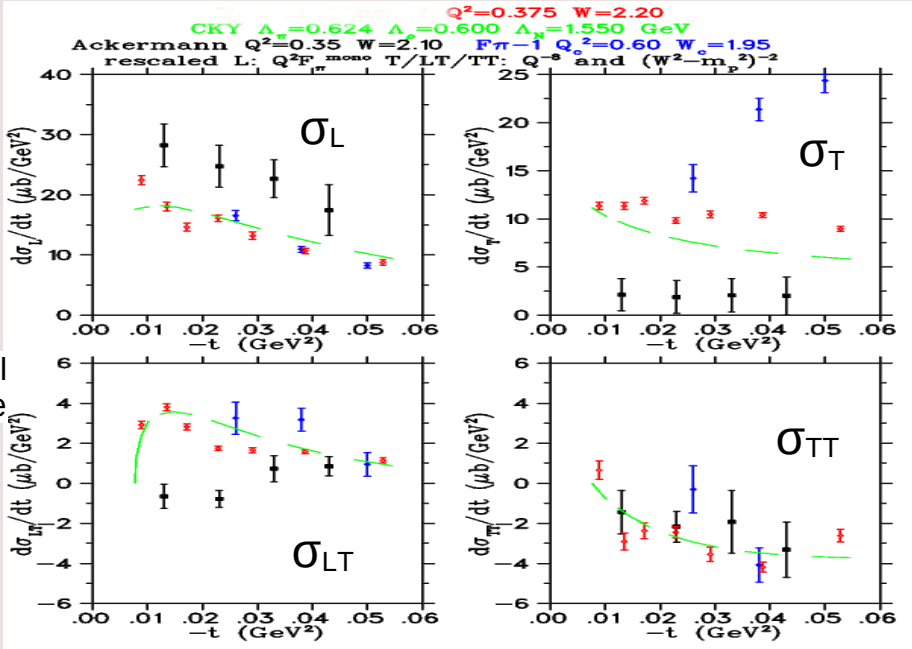

CKY, J. Korean Phys. Soc. 67, L1089 (2015)

Separated X-Sections at Q^2 = 0.425 GeV^2

$$e + p \rightarrow e' + \pi^+ + n$$

- Separated cross sections for seven t bins obtained from a simultaneous fit using the Rosenbluth separation technique.

- Ackermann results rescaled to my kinematics for direct comparison (approximate).

VGL Regge model calculation over the t-bin range.

VGL, Phys. Rev. C 57, 1454 (1998)

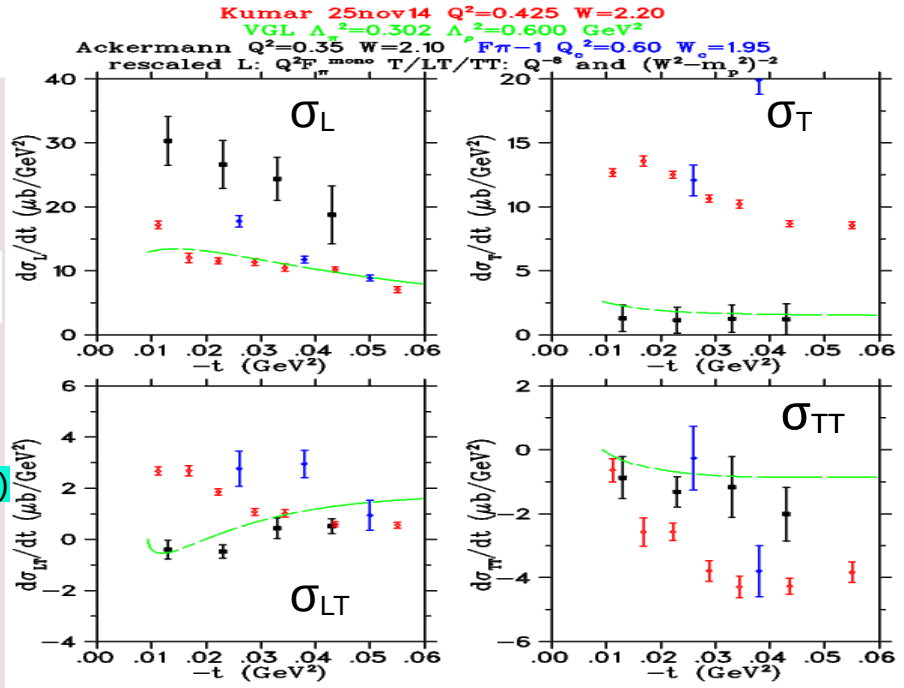

New Findings:

- At Q^2 = 0.35 GeV^2, the Ackermann extraction of σ_{LT} differs in sign, while my results are consistent with the Fπ-1 analysis.

- The VGL model underestimates the σ_T contribution; the CKY model improves the description but does not fully reproduce the data.

- My results and the earlier Fπ-1 analysis show significantly higher σ_T than Ackermann, consistent with the substantial unseparated cross section observed at low ε.

CKY Regge model calculation over the t-bin range.

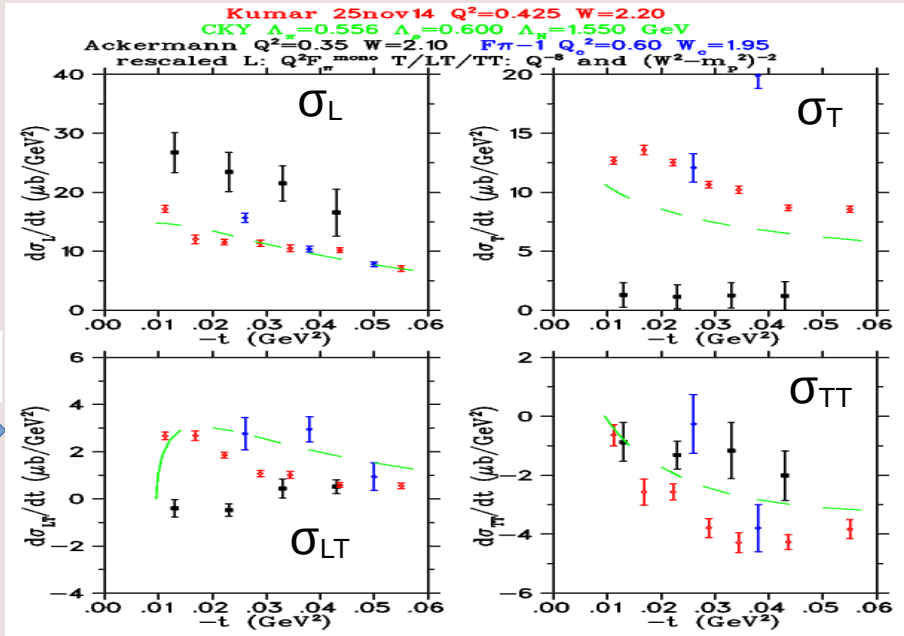

CKY, J. Korean Phys. Soc. 67, L1089 (2015)

New π^+ Form Factor at Q^2 = 0.375 GeV^2!

$$e + p \rightarrow e' + \pi^+ + n$$

- The form factor was extracted from the separated σ_L using the VGL and CKY models at Q^2 = 0.375 GeV^2.
- Extraction of the form factor at Q^2 = 0.425 GeV^2 is still in progress.
- The final PRL publication for this part of the experiment is in progress.

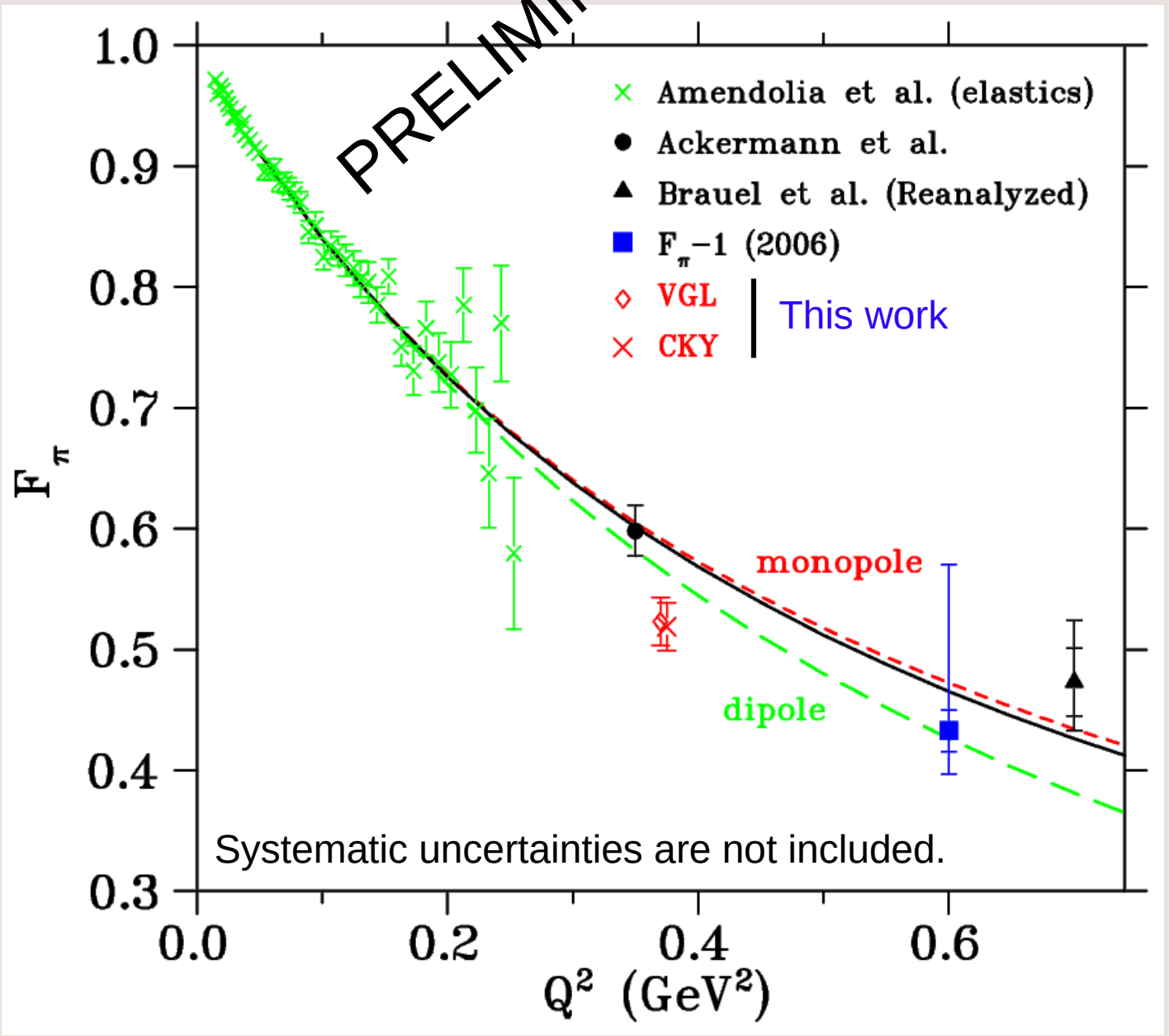

University of Regina

NSERC CRSNG

SAPIN-2021-00026

Thank You!